Optical phonon modes in ordered core-shell CdSe/CdS nanorod arrays

Andrea Giugni,[1] Gobind Das,[1] Alessandro Alabastri,[1] Remo Proietti Zaccaria,[1] Marco Zanella,[1] Isabella Franchini,[1] Enzo Di Fabrizio,[1,2] and Roman Krahne[1,*]

[1]*Italian Institute of Technology (IIT), Via Morego 30, 16163 Genoa, Italy*

[2]*BIONEM Lab, University of Magna Graecia Campus S. Venuta, Germaneto, viale Europa, 88100 Catanzaro, Italy*

(Received 13 January 2012; published 12 March 2012)

We investigate the optical phonons in "dot-in-a-rod" core–shell CdSe/CdS nanorods at wavelengths resonant with the optical transitions either in the core or in the shell. At a wavelength above the CdS band gap, only CdS phonon modes were detected. In contrast, at excitation in resonance with the core transitions, we observed phonon modes of both the CdSe core and the CdS shell. In laterally ordered nanorod assemblies, the CdS longitudinal-optical phonon mode manifested a low-energy shoulder that could be related to higher-order longitudinal-optical phonon modes. Furthermore, we report on surface-optical modes that originate from the tracklike superstructure of the nanorod assemblies.

DOI: 10.1103/PhysRevB.85.115413 PACS number(s): 78.67.Qa, 78.30.Fs, 78.67.Pt

I. INTRODUCTION

Ordered self-assembled nanocrystal arrays are of great interest for both basic science and practical applications. They promise novel physical properties due to collective effects and provide a cost-effective way to fabricate macroscale devices that rely on the peculiar properties of their individual components. Nanorods are especially appealing in this respect because their elongated shape results in distinctive properties like linearly polarized emission and orientation-dependent conductivity, which were observed both on the single particle level[1–3] and on large-scale assemblies.[4–6] Superlattice effects like current oscillations have been detected in tracklike assemblies of CdSe nanorods.[7] The vibrational modes (phonons) of nanocrystals can have significant impact on their optical and electrical response as manifested by phonon replicas in the emission spectrum[8] and by phonon-assisted charge tunneling in electron transport experiments on single nanorods.[9] Optical phonons in colloidal spherical and rod-shaped nanocrystals have been studied in detail, revealing a red-shift and broadening of longitudinal-optical (LO) phonon peak due to confinement effects.[10] Higher harmonics of the LO phonons allowed evaluation of the coupling strength, which is commonly expressed by the Huang-Rhys factor.[11–13] Surface-optical (SO) phonon modes were found to depend on the aspect ratio of the nanorods,[14,15] and radial breathing modes have been observed in both spherical and rod-shaped nanocrystals.[16,17] Linearly polarized Raman experiments on oriented arrays of CdSe nanorods allowed researchers to distinguish LO phonon modes oscillating parallel and perpendicular to the nanorod axis.[14,18] Novel physical properties arising from the superstructure of the ordered nanocrystal assemblies have been reported, for example, by scanning tunneling microscopy, where a reduced band gap was observed in densely packed arrays.[19,20] Core–shell architectures provide a variety of advantages with respect to the optical properties of nanocrystals. The quantum yield of the nanocrystal light emission can be enhanced by passivating the surface of the emitting material with a shell of a higher band gap.[21] Furthermore, the electron and hole wave functions can be engineered via the proper choice of materials and interfaces.[22–24] One popular material for light emitting applications is dot-in-a-rod CdSe/CdS core–shell nanorods fabricated by seeded growth. Here, the emission wavelength can be tuned largely by the size of the core (550–710 nm) and the CdS shell functions as a harvesting antenna for light absorption.[4,25] Temperature-dependent photoluminescence (PL) experiments have demonstrated that the light emission is governed by the CdSe core material.[26]

Here, we investigate optical phonons in core–shell CdSe/CdS nanorods with a dot-in-a-rod architecture that self-assembled into micron-size tracks. Apart from the well-known LO and SO modes previously observed in nanorod homostructures,[14,15] we report the detection of additional modes that could be excited due to the quasi–type II band structure in the core–shell architecture[27] and the tracklike order in the assembly [Fig. 1(a)]. In such samples, we observed not only the fundamental LO phonon modes (with the orbital quantum number $L = 2$) of the CdSe and CdS materials but also the additional LO modes with a higher orbital quantum number that appeared at a slightly lower energy than the fundamental LO phonon mode of the CdS shell. These modes could be detected solely with light excitation in resonance with the excitonic transitions of the CdSe core and were more dominant in ordered tracks with light polarization parallel to the rod axis. They were detected neither in disordered nanorod assemblies nor in ordered assemblies that consisted solely of CdS material. Concerning the SO phonon excitation, the assembly into nanorod tracks gave rise to a new mode whose energy depended on the lateral modulation within the tracks (determined by the nanorod diameter and the thickness of the surfactant layer covering the nanorod surface). Furthermore, the tracklike assembly of the nanorods led to a suppression of the SO phonon mode originating from individual nanorods.

II. EXPERIMENTAL DETAILS

The nanorods were fabricated by the seeded growth method according to Ref. 4. We investigated nanorods with lengths from 30 to 50 nm and core sizes ranging from 2.5 to 3.2 nm. We present in the following the data obtained from a representative nanorod sample, which had a diameter of 5 nm and a length of 40 nm. Data obtained from another nanorod sample with a

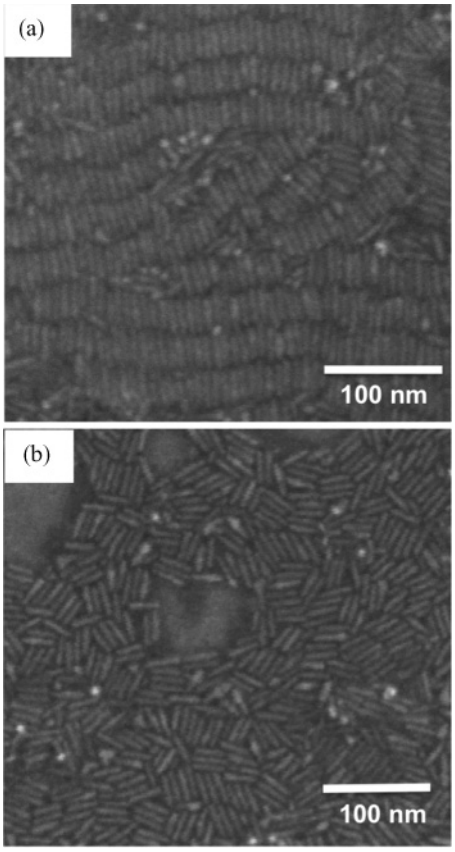

FIG. 1. (a) Scanning electron microscopy (SEM) image of nanorod tracks formed by drop deposition of the nanorod solution on a Si substrate followed by solvent evaporation under ambient conditions. (b) SEM image of disordered nanorods.

smaller length of 30 nm are reported in the supplementary material.[28] Optical absorption and emission spectra were recorded from nanorods in solution with a commercial spectrophotometer. For the Raman experiments, nanorods dissolved in toluene (at a concentration of 10^{-6} M) were drop-casted onto planar substrates (Si or CaF_2), followed by slow evaporation of the solvent under ambient conditions, which led to the lateral (side-to-side) assembly of the nanorods into micron-size tracks [Fig. 1(a)]. Such tracks represent a nanorod superlattice in which the lattice period is determined by the rod diameter and the length of the surfactants that coat the lateral facets. Reference samples with disordered nanorod ensembles were obtained by spin-coating the nanorod solution at 3000 rpm for 60 s onto the substrates [Fig. 1(b)]. Microprobe Raman (Horiba, T64000, in subtractive configuration) experiments were performed under ambient conditions using an Argon-krypton ion laser (Spectra-Physics, Ar:Kr Stabilite 2018-RM) at 458 and 514 nm. The inelastic scattered radiation from the substance was filtered by triple monochromator, equipped with 1800 lines/mm grating, and the output signal was detected by a Peltier-cooled charge-coupled device detector. The samples were mounted on an inverted microscope (Olympus, IX71), and an aplanatic, infinity-corrected microscope objective 100× (Olympus, UPLSAPO) was employed to focus laser excitation to a diffraction-limited spot and to collect the back-scattered Raman signal.

III. EXPERIMENTAL RESULTS AND DISCUSSION

Absorption and emission spectra recorded from core–shell nanorods in solution are reported in Fig. 2. Gaussian fits to the relevant sections of the absorption spectrum revealed the lowest absorption peak of the CdSe core at 595 nm and of the CdS shell at 455 nm. The emission peak at 630 nm is red-shifted with respect to the CdSe core absorption due to the Stokes shift.[4,29] The excitation wavelengths employed in the Raman experiments are indicated by the black, vertical lines. The inset of Fig. 2 illustrates the core–shell architecture, in which a spherical CdSe core is embedded in a rod-shaped CdS shell, as well as the related band structure, where we assumed strong confinement for the holes in the valence band (VB) and a negligible offset in the conduction band (CB).[23,27]

Excitons and phonons in polar materials such as CdSe and CdS couple predominantly via the Fröhlich interaction, which for LO phonons can be approximated by the interaction of the phonons with a static charge distribution. In particular, the Raman cross section for an nth-order phonon process can be expressed as[11,13,30]

$$|R^{(n)}(\omega)|^2 = \mu^4 \left| \sum_{m=0}^{\infty} \frac{\langle n|m\rangle\langle m|0\rangle}{E_{ij} + n\cdot\hbar\omega_{\mathrm{LO}} - \hbar\omega + i\hbar\Gamma} \right|^2 \quad (1)$$

where E_{ij} is the exciton excited state energy, μ is the dipole matrix element between the electronic ground and excited state, m is an intermediate vibrational level, and Γ is the homogeneous linewidth. We can derive the resonant behavior of the Raman signal with the excitonic transitions from the denominator in Eq. (1), and those transitions in our case can be related to either the CdSe core or the CdS shell, as highlighted in Fig. 2. Therefore, at the excitation wavelength $\lambda 1 = 458$ nm, the Raman signal is in resonance with the transitions in the nanorod shell (CdS), while at $\lambda 2 = 514$ nm,

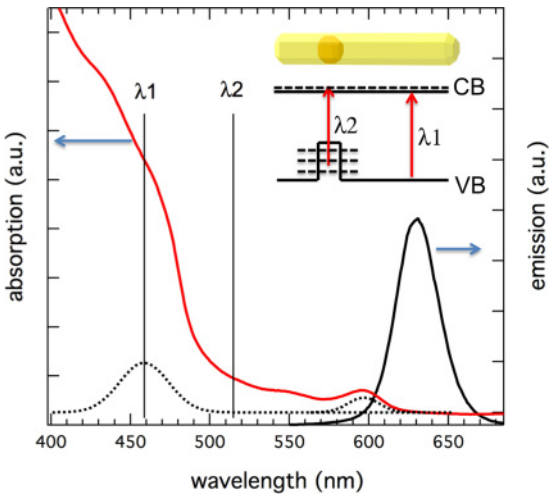

FIG. 2. (Color online) Absorption and emission spectra of CdSe/CdS nanorods recorded from solution. Gaussian fits to the first absorption peaks from the CdSe core and CdS shell are shown by the dotted lines. The two excitation wavelengths for the Raman experiments ($\lambda 1 = 458$ nm and $\lambda 2 = 514$ nm) are marked by the vertical lines. The inset illustrates the dot/rod core–shell architecture and the related band structure of the nanorods. At a wavelength of 514 nm, only transitions related to the CdSe are possible.

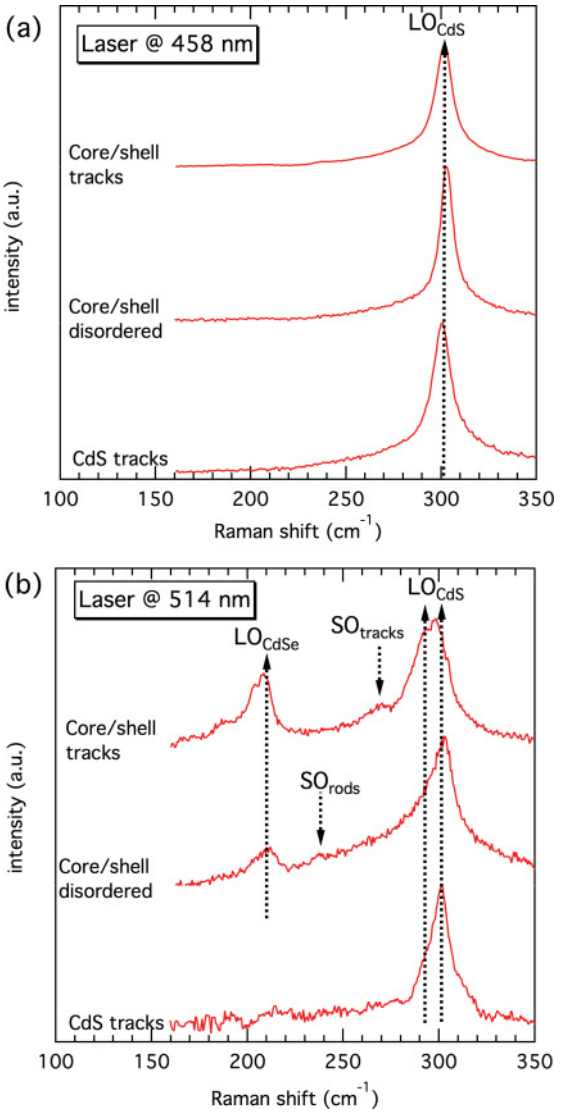

FIG. 3. (Color online) Raman spectra recorded from different nanorod films at excitation wavelengths of (a) 458 nm and (b) 514 nm. (a) The excitation corresponds to transitions of the CdS shell, and solely the CdS phonon modes can be observed from the ordered, disordered, and CdS nanorod films. (b) For a laser wavelength of 514 nm, in resonance with the core transitions, the CdSe LO phonon can be observed from the core–shell rods. In particular, additional SO and LO phonon modes in the CdS band appear in the spectrum recorded from the nanorod tracks. The arrow labeled SO_{rods} indicates the calculated energy for the fundamental SO phonon mode in nanorods with an aspect ratio of 1/8 (see Eq. (2) and data on CdSe in Ref. 14).

it is in resonance with transitions related to excited states in the CdSe core[4] (see the red arrows in the inset of Fig. 2). Furthermore, the dependence on the dipole matrix element μ has some impact on polarization-dependent measurements on oriented assemblies of anisotropic nanocrystal structures like nanorods, as discussed later.

Figure 3 shows Raman spectra recorded from highly ordered and disordered nanorod ensembles at excitation wavelengths of $\lambda 1 = 458$ nm [Fig. 3(a)] and $\lambda 2 = 514$ nm [Fig. 3(b)]. In the case of excitation at 458 nm, i.e., in resonance

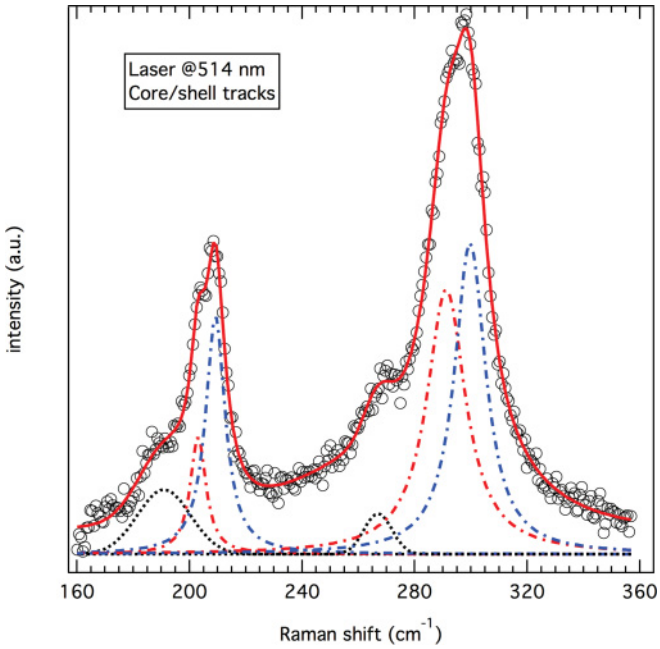

FIG. 4. (Color online) Lorentzian fits (red and blue dashed-dot) to the LO phonon modes and Gaussian fits (black dotted) to the Raman spectrum (open circles) recorded from core–shell nanorod tracks at an excitation wavelength of 514 nm [the same as in Fig. 3(b)]. The resulting fit to the data is shown by the solid (red) line. The obtained peak positions are 300 cm^{-1} for CdS(LO$_1$), 291 cm^{-1} for CdS(LO$_2$), 267 cm^{-1} for CdS(SO), 209 cm^{-1} for CdSe(LO$_1$), 203 cm^{-1} for CdSe(LO$_2$), and 191 cm^{-1} for CdSe(SO).

with the CdS shell states, we observed the fundamental CdS LO phonon mode at 302 cm^{-1}, which slightly red-shifted from the CdS bulk value (305 cm^{-1})[31] due to confinement effects.[10] The Raman signal recorded from the ordered, disordered, and CdS-only samples does not show significant differences at this excitation energy. Also the first overtone of the CdS LO phonon at 604 cm^{-1} could be observed (see supplemental material[32]). Raman spectra at 514 nm, in resonance with the higher exciton transitions of the CdSe core, are depicted in Fig. 3(b). Here, the CdSe LO phonon manifested due to the resonance of the laser excitation with the core transitions. In addition, the CdS phonon modes were detected with a comparable or even stronger signal than the CdSe ones at this excitation energy, which can be related to the delocalization of the electrons into the rod-shaped CdS shell. The most intriguing features in the spectrum of the ordered rod assembly in Fig. 3(b) are (1) the additional peaks on the low-energy side of the fundamental CdS LO phonon mode marked by the arrow and (2) the broad mode that appeared at 270 cm^{-1}. Interestingly, these additional modes appeared in the energy band of the CdS phonons but were in resonance with electronic excitations related to the CdSe core. Both features depended on the degree of order in the nanorod assemblies and were not detected from pure CdS nanorod samples. Furthermore, they were solely observed at laser excitation wavelengths well below the CdS band gap.

The results obtained from fitting the LO phonon modes with Lorentzian curves and the SO phonon modes with Gaussian curves are displayed in Figure 4. The fitting reveals that the CdS LO phonon mode is composed of two peaks

with comparable amplitude and that the CdSe LO phonon band is composed of two peaks. Furthermore, we observed a broad peak centered at 267 cm^{-1} that can be attributed to a superlattice CdS SO phonon mode in the nanorod tracks, as argued in detail in Sec. III B. At 191 cm^{-1}, we observed the SO phonon mode of the CdSe cores, in excellent agreement with the energy calculated from Eq. (2) for a spherical particle (aspect ratio = 1) and considering CdS as the dielectric environment that yields a value of 190 cm^{-1}. The energy of the CdSe LO phonon is red-shifted from that of CdSe nanorods[14] due to the stronger confinement, and our findings in the CdSe phonon band are in good agreement with those presented in Ref. 13.

A. Discussion of LO phonon modes

To gain more information on the LO phonon modes, we performed polarization-dependent measurements. The amount to which the PL amplitude depends on the angle of polarization of the linearly polarized laser excitation can give a measure for the degree of nanorod alignment within the laser spot area, and a large PL amplitude corresponds to light polarization parallel to the long nanorod axis.[4,25] The inset of Fig. 5(a) shows the different signal intensities in the onsets of the PL emission

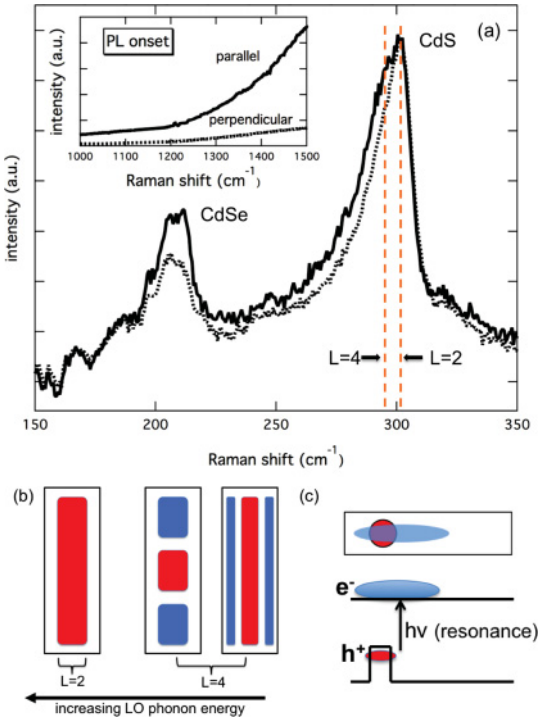

FIG. 5. (Color online) (a) Raman spectra recorded from core–shell nanorod tracks with light excitation at 514 nm for two perpendicular laser polarizations, parallel (solid line) and perpendicular (dotted line) to the long nanorod axis. The Raman spectra were normalized with respect to the amplitude of the CdS LO phonon peak. Clearly, the spectral shape depended on the polarization. The inset shows the signal amplitude at the onset of the PL peak. The displayed window corresponds to the spectral range of 557–542 nm. (b) Sketch of phonon potentials for the LO modes in nanorod homostructures with orbital quantum numbers $L = 2$ and $L = 4$. (c) Localization of the electrons (e, blue/light gray) and holes (h, red/dark gray) for an excitation wavelengths of 514 nm.

for two perpendicular laser polarizations for a fixed spot area and size, confirming a high degree of nanorod alignment.[4] The corresponding Raman spectra show the double-peak structure in the LO phonon band of the CdS. We clearly observe a systematic change in shape in the spectra with respect to the incident laser polarization. For polarization parallel to the long nanorod axis (called parallel polarization in the following), an additional peak at the low-energy side of the CdS phonon peak can clearly be evidenced in the spectrum. This peak is much weaker in perpendicular polarization.

Previous works on LO phonon excitation in nanorod homostructures reported the excitation of phonon modes with higher orbital quantum numbers.[14] The phonon potentials of the modes with even orbital quantum numbers $L = 2$ and $L = 4$ are depicted in Fig. 5(b). We remark that only modes with even L are allowed by the selection rules for Raman scattering. It is reasonable to assume that the polarization-dependent shape of the CdS LO phonon band can be related to the different anisotropy of the phonon modes with higher orbital quantum numbers, which is either parallel or perpendicular to the long nanorod axis. Figure 5(b) illustrates the potentials of LO phonon modes with orbital quantum numbers $L = 2$ and $L = 4$ (red/dark gray for high and blue/light gray for low potential) following the theory of Refs. 14 and 33. In aligned arrays of homostructure CdSe nanorods, the first $L = 4$ mode was observed in perpendicular polarization due to its higher symmetry in this direction (see Ref. 14). In our case of dot/rod core–shell nanorods, with excitation energies below the CdS band gap, the photoexcited holes are localized to the CdSe core region, while the electrons are more delocalized over the CdS rod volume.[23,27] Figure 5(c) illustrates this spatial distribution of the electrons and holes in the core–shell nanorods that results from the different band offsets in the CB and VB. This asymmetry in charge distribution along the long nanorod axis, on the one hand, results in a stronger dipole matrix element in parallel polarization (and therefore increases the Raman cross section) and, on the other hand, is not compatible with the symmetry of the second $L = 4$ phonon potential sketched in Fig. 5(b), which is elongated along the long nanorod axis. It is therefore reasonable to assume that the first $L = 4$ mode is enhanced in parallel polarization, leading to a stronger signal of the peak at 291 cm^{-1}.

B. Discussion of SO phonon modes

We now show that the broad mode that manifested at 267 cm^{-1} (CdS(SO)) observed in the nanorod tracks) can be related to a SO phonon excitation of the nanorod tracks. Figure 6 shows the SO phonon energy calculated according to the model introduced by Gupta *et al.*[34] for GaP nanowires that could be adapted for SO phonons in colloidal nanorods.[14] In this approach, the SO phonon energy for a wirelike nanostructure is expressed in terms of a dimensionless parameter $x = q \cdot r$. Here, r is the radius of the nanowire and q is the momentum transferred along the nanowire, which can be provided either by a periodic modulation of the nanowire diameter or by the finite length of the nanorods. The energy of the SO phonon modes can then be written as

$$\omega_{SO}^2 = \omega_{TO}^2 + \frac{\varepsilon_\infty(\omega_{LO}^2 - \omega_{TO}^2)}{\varepsilon_\infty + \varepsilon_M f(x)} \qquad (2)$$

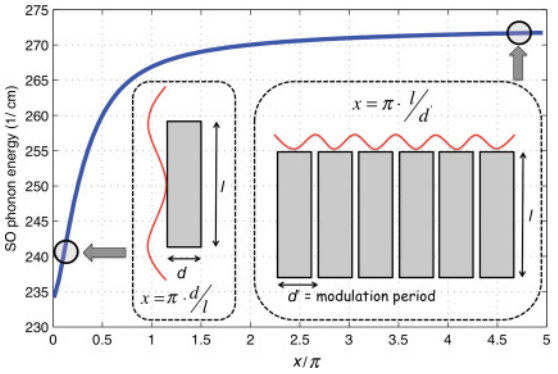

FIG. 6. (Color online) SO phonon dispersion versus the parameter x/π that enters in Eq. (2). The two circles indicate the SO phonon energy for disordered samples (bottom left) and nanorod tracks (top right). The red wavy lines in the insets illustrate the SO phonon potential for a single rod (right) and a nanorod track (left), together with Eqs. (4) and (5) for x. In the tracks, $d + \sigma = d'$.

where $\varepsilon_\infty = 5.23$ is the high-frequency dielectric constant of CdS, ε_M is the dielectric constant of the surrounding medium (approximated by $\varepsilon_M = 4$ as average value of an environment consisting of empty space, organics like the surfactants that cover the nanorod surface, and neighboring nanorods), and $\omega_{TO} = 234$ cm^{-1} and $\omega_{LO} = 305$ cm^{-1} are the TO and LO phonon energies in CdS, respectively.[31] In addition,

$$f(x) = I_0(x) \cdot K_1(x)/[I_1(x) \cdot K_0(x)], \tag{3}$$

with I and K as Bessel functions. We emphasize that for a single nanorod, the momentum vector in direction of the long nanorod axis can be provided by the finite nanorod length. Therefore,

$$q = 2\pi/l \quad \text{and} \quad r = d/2; \quad \text{thus,} \quad x = \pi \cdot d/l, \tag{4}$$

where d is the diameter of the rod and l is its length.

However, the momentum vector q in the nanorod tracks results from the periodic modulation along the lateral sides of the tracks, as illustrated in the inset in Fig. 6, and can be expressed as

$$q = 2\pi/(d+\sigma) \quad \text{and} \quad r = l/2, \quad \text{which leads to} \quad x = \pi \cdot l/(d+\sigma), \tag{5}$$

with σ being the thickness of the surfactant layer covering the lateral nanorod facets. The insets of Fig. 6 illustrate these two configurations that result in significantly different SO phonon energies, i.e., $\sim$240 cm^{-1} for single rods and $\sim$270 cm^{-1} for nanorod tracks [as evidenced in the core–shell nanorod "tracks" spectrum in Fig. 3(b)]. Furthermore, we expect the neighboring nanorods in the tracks to cause a suppression of the SO phonon mode originating from individual nanorods due to the significant extension of the SO phonon potential in the region outside the nanocrystal structure.[14] We do not observe any excitation $\sim$240 cm^{-1} in the spectra from the tracks in Fig. 3. From the point of view of SO phonons, the nanorod tracks resemble micron-size nanowires with a diameter equal to the nanorod length and a lateral modulation on the length scale of the nanorod diameter that provides the necessary q vector. Our model seems to describe the SO phonon behavior of the nanorod tracks quite well, although it does not consider the inhomogeneous nature within the nanorod assembly.

IV. CONCLUSIONS

We observed optical phonon excitations from both core and shell materials in dot-in-a-rod core–shell nanorods by Raman spectroscopy. Interestingly, the CdS LO phonon could be excited in resonance with the CdSe core transitions, which can be rationalized by the electron delocalization of the CdSe exciton states into the rod shell. This peculiar charge distribution in the core–shell nanorods allowed coupling to LO phonon modes with a higher-order quantum number L. The tracklike self-assembly of the nanorods enhanced the possibility for detection of these higher LO phonon modes from micron-size areas. Furthermore, nanorod tracks showed a novel SO phonon mode originating from the superstructure that resulted from their side-by-side self-assembly.

*roman.krahne@iit.it

[1] J. T. Hu, L. S. Li, W. D. Yang, L. Manna, L. W. Wang, and A. P. Alivisatos, Science **292**, 2060 (2001).
[2] P. E. Trudeau, M. Sheldon, V. Altoe, and A. P. Alivisatos, Nano Lett. **8**, 1936 (2008).
[3] H. Steinberg, Y. Lilach, A. Salant, O. Wolf, A. Faust, O. Millo, and U. Banin, Nano Lett. **9**, 3671 (2009).
[4] L. Carbone, C. Nobile, M. De Giorgi, F. D. Sala, G. Morello, P. Pompa, M. Hytch, E. Snoeck, A. Fiore, and I. R. Franchini *et al.*, Nano Lett. **7**, 2942 (2007).
[5] D. Steiner, D. Azulay, A. Aharoni, A. Salant, U. Banin, and O. Millo, Phys. Rev. B **80**, 195308 (2009).
[6] A. Persano, M. De Giorgi, A. Fiore, R. Cingolani, L. Manna, A. Cola, and R. Krahne, ACS Nano **4**, 1646 (2010).
[7] H. E. Romero, G. Calusine, and M. Drndic, Phys. Rev. B **72**, 235401 (2005).
[8] D. J. Norris, A. L. Efros, M. Rosen, and M. G. Bawendi, Phys. Rev. B **53**, 16347 (1996).
[9] Z. X. Sun, I. Swart, C. Delerue, D. Vanmaekelbergh, and P. Liljeroth, Phys. Rev. Lett. **102**, 196401 (2009).
[10] C. Trallero-Giner, A. Debernardi, M. Cardona, E. Menendez-Proupin, and A. I. Ekimov, Phys. Rev. B **57**, 4664 (1998).
[11] A. P. Alivisatos, T. D. Harris, P. J. Carroll, M. L. Steigerwald, and L. E. Brus, J. Chem. Phys. **90**, 3463 (1989).
[12] R. Krahne, G. Chilla, C. Schuller, L. Carbone, S. Kudera, G. Mannarini, L. Manna, D. Heitmann, and R. Cingolani, Nano Lett. **6**, 478 (2006).
[13] H. Lange, M. Artemyev, U. Woggon, T. Niermann, and C. Thomsen, Phys. Rev. B **77**, 193303 (2008).
[14] C. Nobile, V. A. Fonoberov, S. Kudera, A. Della Torre, A. Ruffino, G. Chilla, T. Kipp, D. Heitmann, L. Manna, R. Cingolani *et al.*, Nano Lett. **7**, 476 (2007).

[15]H. Lange, M. Artemyev, U. Woggon, and C. Thomsen, Nanotechnology **20**, 045705 (2009).
[16]G. Chilla, T. Kipp, T. Menke, D. Heitmann, M. Nikolic, A. Fromsdorf, A. Kornowski, S. Forster, and H. Weller, Phys. Rev. Lett. **100**, 057403 (2008).
[17]H. Lange, M. Mohr, M. Arternyev, U. Woggon, and C. Thomsen, Nano Lett. **8**, 4614 (2008).
[18]G. D. Mahan, R. Gupta, Q. H. Xiong, C. K. Adu, and P. C. Eklund, Phys. Rev. B **68**, 073402 (2003).
[19]D. Steiner, A. Aharoni, U. Banin, and O. Millo, Nano Lett. **6**, 2201 (2006).
[20]D. Steiner, D. Azulay, A. Aharoni, A. Salant, U. Banin, and O. Millo, Nanotechnology **19**, 065201 (2008).
[21]P. Reiss, M. Protiere, and L. Li, Small **5**, 154 (2009).
[22]A. Fiore, R. Mastria, M. G. Lupo, G. Lanzani, C. Giannini, E. Carlino, G. Morello, M. De Giorgi, Y. Q. Li, R. Cingolani *et al*., J. Am. Chem. Soc. **131**, 2274 (2009).
[23]A. Sitt, F. D. Sala, G. Menagen, and U. Banin, Nano Lett. **9**, 3470 (2009).
[24]M. T. Trinh, L. Polak, J. M. Schins, A. J. Houtepen, R. Vaxenburg, G. I. Maikov, G. Grinbom, A. G. Midgett, J. M. Luther, M. C. Beard *et al*., Nano Lett. **11**, 1623 (2011).
[25]D. V. Talapin, R. Koeppe, S. Gotzinger, A. Kornowski, J. M. Lupton, A. L. Rogach, O. Benson, J. Feldmann, and H. Weller, Nano Lett. **3**, 1677 (2003).
[26]G. Raino, T. Stoferle, I. Moreels, R. Gomes, J. S. Kamal, Z. Hens, and R. F. Mahrt, ACS Nano **5**, 4031 (2011).
[27]M. G. Lupo, F. Della Sala, L. Carbone, M. Zavelani-Rossi, A. Fiore, L. Luer, D. Polli, R. Cingolani, L. Manna, and G. Lanzani, Nano Lett. **8**, 4582 (2008).
[28]See Supplemental Material at http://link.aps.org/supplemental/10.1103/PhysRevB.85.115413 for data obtained from another nanorod sample with a smaller length of 30 nm.
[29]A. L. Efros, M. Rosen, M. Kuno, M. Nirmal, D. J. Norris, and M. Bawendi, Phys. Rev. B **54**, 4843 (1996).
[30]R. Merlin, G. Guntherodt, R. Humphreys, M. Cardona, R. Suryanarayanan, and F. Holtzberg, Phys. Rev. B **17**, 4951 (1978).
[31]*Landolt-Boernstein, Group II Condensed Matter*, Vol. 41b (Springer-Verlag, Berlin, 1998).
[32]See Supplemental Material at http://link.aps.org/supplemental/10.1103/PhysRevB.85.115413 for Raman spectra showing the first overtone of the CdS LO phonon at 604 cm^{-1} (Fig. S2).
[33]V. A. Fonoberov and A. A. Balandin, J. Phys. Condens. Matter **17**, 1085 (2005).
[34]R. Gupta, Q. Xiong, G. D. Mahan, and P. C. Eklund, Nano Lett. **3**, 1745 (2003).